Physica B 192 (1993) 137–149
North-Holland

SDI: 0921-4526(93)E0120-6

PHYSICA B

Magnetic depth profiling studies by polarized neutron reflection

G.P. Felcher

Argonne National Laboratory, Argonne, IL, USA

A review is given of the role of polarized neutron reflectivity (PNR) in measuring the magnetic profile close to the surface and in thin films of superconductors and magnetic materials. For type I and type II superconductors PNR provided a new and direct determination of the penetration depth. For very thin ferromagnetic films PNR was able to determine the absolute value of the magnetic moments. In magnetic superlattices, formed by the alternation of ferromagnetic layers and nonmagnetic spacers, PNR was used to confirm the basic magnetic structure as well as to determine the direction of the magnetic moments of the individual layers. In addition to reflectivity, forward magnetic scattering may very well extend the usefulness of PNR to the case of laterally dishomogeneous systems.

1. Reflectivity from magnetic layers

Polarized neutron reflectivity (PNR) has blossomed in recent years, because it is a simple method to measure the magnetic depth profile of thin films and in proximity of the surface and of interfaces. Neutron reflectivity is an optical technique: thus the interaction of neutrons with matter, which gives rise to reflection, is approached in a form slightly different from the conventional treatment of neutron scattering. When neutrons propagate through a medium in which the scattering centers are small compared with the neutron wavelength, the effect of the medium may be represented by a smooth pseudopotential whose magnitude is related simply to the scattering density and the magnetic induction in the material [1] as

$$V_{\text{eff}} \quad V_{\text{n}} + V_{\text{m}} = \frac{2\pi\hbar^2}{m} bN + \boldsymbol{B}\cdot\hat{s}$$

where b is the sum of all the scattering lengths over the N atoms occupying a unit volume. If the potential is a function only of the depth from the surface (as in a stratified medium) the Schröding-

Correspondence to: G.P. Felcher, MSD-223, Argonne National Laboratory, Argonne, IL 60439, USA.

er equation for the neutron may be separated in cartesian coordinates. Practically only the z component of the motion needs to be considered: in the plane (x, y) (parallel to the surface) the motion is that of a free particle and the corresponding components of the wavevector are constant. The two spinor components $\psi_+(z)$, $\psi_-(z)$ of the neutron wave function obey, at a depth z in the medium, the Schrödinger equations [2,3]:

$$\begin{aligned}
&\frac{\hbar^2}{2m}\left(\frac{\mathrm{d}^2\psi_+}{\mathrm{d}z}\right. + (V_{\text{n}} + 2\mu_{\text{n}}B_{\parallel})\psi_+ \\
&+ 2\mu_{\text{n}}B_{\perp}\psi_- \quad \frac{\hbar^2 k_z^2}{2m}\psi_+ \\
&\left(\frac{\hbar^2}{2m}\right)\left(\frac{\mathrm{d}^2\psi_-}{\mathrm{d}z^2}\right) + (V_{\text{n}} - 2\mu_{\text{n}}B_{\parallel})\psi_- \\
&+ 2\mu_{\text{n}}B_{\perp}\psi_+ = \frac{\hbar^2 k_z^2}{2m}\psi_-
\end{aligned} \qquad (2$$

where $k_z = 2\pi(\sin\theta_{\text{i}}/\lambda)$ is the component of the momentum of the incident neutron normal to the surface, θ_{i} the angle of incidence, λ the neutron wavelength and μ_{n} its magnetic moment.

The z-axis is chosen to point from the vacuum toward the surface which is placed at $z = 0$. The wavefunction in the halfspace $z < 0$ is

$$\psi_+ = \exp(ik_z \cdot z) + R_{++} \exp(-ik_z \cdot z)\,,$$
$$\psi_- = R \quad \exp(\ ik \quad z)\,, \tag{3}$$

for an incoming wavefunction fully polarized in the + state. If at depths greater than z_F the refractive index becomes constant and nonmagnetic the wavefunction can be described [4] by

$$\psi_+ = T_{++} \exp(ik_{F+}z)\,,$$
$$\psi_- = T_+ \quad \exp(ik_{F-}z)\,, \tag{4}$$

where

$$k \quad \sqrt{k_z^2 - 4\pi(bN \pm cB_T)}\,, \quad B_T = \sqrt{B_\parallel^2 + B_\perp^2} \tag{5}$$

The conditions of continuity of the wave function and of its derivative at all values of z allow the determination of $R_{++}, R_{+-}, T_{++}, T_{+-}$, and of the reflectivities $|R_{++}|^2$ and $|R_{+-}|^2$, which are most directly compared with the experimental quantities.

If the sample magnetization is parallel to an applied magnetic field $\boldsymbol{H}$ (which is also the quantization axis of the neutron) the two eqs. (2) do not contain crossterms. The neutron spin in its trajectory remains in its original state, either parallel to $\boldsymbol{H}$ (+), or opposite to it (−). Figure 1 shows a typical example [5] of spin-dependent reflectivities for a 300 Å layer of permalloy on the top of an antiferromagnetic film of $Ni_{0.5}Co_{0.5}O$. Basically the reflectivity $|R^+(k_z)|^2$ is an optical transform of $b(z)N(z) + cB(z)$ and similarly $|R^-(k_z)|^2$ is an optical transform of $b(z)N(z) - cB(z)$. Much work has been done recently [6,7,8] to find the optimal way to execute this transform which, for large values of k_z, reduces to a Fourier transform. To present in more concise form the magnetic information of the reflectivity quantities such as $|R^+|^2/|R^-|^2$ have been introduced, conventionally named 'flipping ratio'. More recently it has been preferred to present the data as $P = (R^+ - R^-)/(R^+ + R^-)$; this is called 'polarization' or 'spin asymmetry'. When $\boldsymbol{B}_\perp \neq 0$, analysis of the polarization of the reflected beam gives a spin-flip

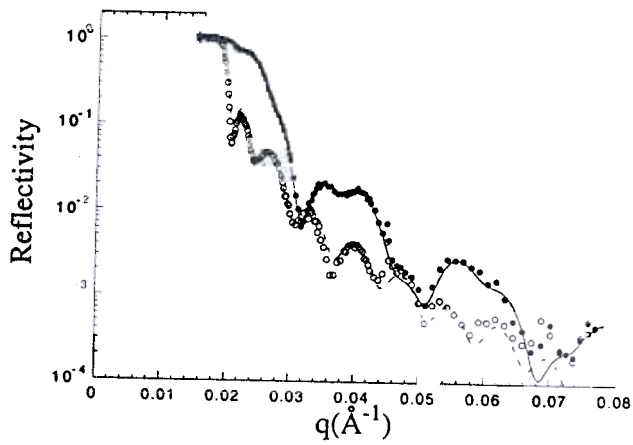

Fig. 1. Polarized neutron reflectivity of a film of permalloy on $Ni_{0.5}Co_{0.5}O$, at a temperature of 20 K. The abscissa is $q = 2k_z$. The permalloy is magnetized in the direction of the applied field H. Full points: neutrons polarized parallel to H (R^+). Open circles: neutrons polarized opposite to H (R^-) (see ref. [5]).

reflectivity, $|R_{+-}|^2 = |R_{-+}|$, which is an optical transform of $\boldsymbol{B}_\perp(z)$.

Figure 2 shows pictorially some of the cases that can be encountered [9]. The + and − signs refer to the relative polarizations of the neutron spin with respect to the applied magnetic field H, which acts as a quantization axis for the polarized neutrons. When a ferromagnetic layer is magnetically saturated in the plane of the film along the direction of H, the neutrons remain polarized during the reflection process (fig. 2(a)). If instead the direction of the magnetization deviates from the quantization axis, the neutrons undergo a partial precession during the reflection process, so that the reflected beam appears as partially depolarized (fig. 2(b)). If the ferromagnetic film is not saturated, but for simplicity the magnetization is uniaxial, the sample is divided in magnetic domains aligned either parallel or antiparallel to the applied field. In this case there is no depolarization of the reflected beam, but the values of $|R_+|^2$ and $|R_-|^2$ represent a weighted average over the reflectivities of the individual domains (fig. 2(c)). Finally, if H is applied perpendicular to the film and is sufficiently large to magnetize the sample in that direction, the neutron reflectivities become optical transforms of the nuclear profile only (fig. 2(d)). This is

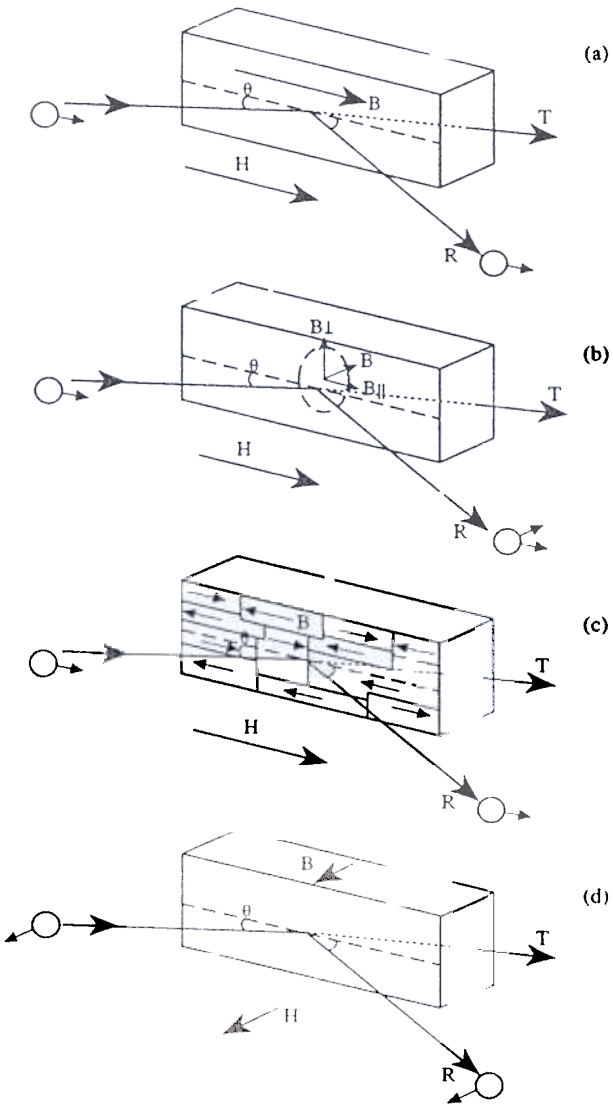

Fig. 2. Effects of the film magnetization on the neutron reflectivity and polarization. In configurations (a) and (b) the reflectivity is spin-dependent; however, in (b) the spin of the reflected beam is partially rotated. For (c) the reflectivity is average for that of the two neutron spin states while for configuration (d) the reflectivity is due only to nuclear interactions (see ref. [9]).

because B_z, the component of $\boldsymbol{B}$ normal to the surface, is continuous across the surface.

Conceptually (and to a great deal even practically) a reflectometer is a very simple instrument. A narrow beam of neutrons of wavelength λ hits a sample surface at an angle θ (of the order of one degree) and is reflected at the same angle θ into the detector. Appropriate devices polarize the neutrons before the sample in the direction parallel to an applied magnetic field or opposite to it. Similar devices, if inserted in the neutron path after reflection of the sample, allow polarization analysis. Reflectometers have been constructed at both steady-state [10] and pulsed neutron sources [2,11,12,13]. At steady state sources the reflectivity as a function of $k_z = 2\pi \sin\theta/\lambda$ is obtained in the following way. The neutron beam is monochromatized to a wavelength λ_0. A suitable region of k_z is spanned by varying the angle θ between beam and sample surface (and sample surface/detector). In contrast, at pulsed sources all the neutrons contained in the source spectrum are utilized, and their wavelength is sorted out by the time of flight from source to detector. Here a substantial region of k_z is covered without changing the angle of incidence θ. In all cases the maximum value of k_z spanned determines the resolution length Δz in direct space: $k_z \sim 1/\Delta z$.

Both types of instruments have distinct advantages. At a steady-state source one can choose the k_z region of interest with great flexibility, taking data only where needed and with the desired statistics. The neutron wavelength may be chosen at the top of the maxwellian which characterizes the neutron spectrum. The resolution,

$$[\Delta k \quad k_z]^2 = [\Delta\theta/\theta] \quad [\Delta\lambda/\lambda]^2$$

consists of two terms of comparable size which do not vary greatly with angle. This means that high resolution can be obtained at large angle. On the other hand, the instruments at pulsed sources have their own advantages: they permit the observation of the entire reflectivity pattern *at once*; the footprint of the beam on the sample is fixed; since $\Delta k_z/k_z \sim \Delta\lambda/\lambda$ is constant the resolution is excellent for k_z values close to the region of total reflection. The choice of the 'best' instrument is thus dictated by the experiment to be performed.

The review presented here covers only the PNR work done in selected areas of research where rapid development is taking place. The list is not all-inclusive. For instance, PNR has been used to study the effects of thermal and chemical

treatment on the surface magnetism of ferrites [14]. It has also been used to study the magnetic depth profiles of relatively thin films, when deposited either on grossly mismatched lattices (like strained layers of Fe and Co on GaAs) [15], or on antiferromagnetic substrates (like permalloy on NiO) [5,9] which provide a unidirectional bias.

2. Superconductivity

The magnetic state of a body is always perturbed at the surface, and the perturbation extends over a thickness that depends on the range of the interaction forces. In a ferromagnet, at $T = 0$ the magnetic moments are significantly different from the bulk value up to three atomic planes from the surface. Such distance is too short to be detectable by reflectivity at present day neutron sources. The thickness of the 'magnetic surface layer' increases with the temperature [16] and actually becomes infinite at the magnetic transition temperature. However, in practice the span of temperatures over which surface effects become visible is small and attempts made up to now [17] have not provided reliable values for the critical exponents. More promising is the case of superconductors.

As is well known [18], magnetic fields always penetrate to some extent the surface of a superconducting material. For an applied field H less than a critical field (the thermodynamic critical field H_c for type-I superconductors; the lower critical field H_{c1} for type-II superconductors) the penetration is restricted to a depth of the order of a few hundred Ångstroms. At higher field the penetration is more dramatic: for instance for type-II superconductors, in fields between H_{c1} and H_{c2} (the upper critical field) a mixed state of quantized vortex lattice has been observed both by small angle neutron diffraction and decoration techniques utilizing small magnetic particles. There are two situations that are strictly surface effects and cannot be conveniently studied by the preceding techniques. These are the Meissner state, in which the field penetrates only a small distance into the superconductor, and the surface sheath, in which superconductivity and diamagnetism exist only in a shallow surface layer when the field is applied parallel to the plate. The latter state occurs between H_{c2} and a surface nucleation field H_{c3}.

Only a few experiments have been made on superconductors (mostly below H_{c1}) and yet there is a fair amount of disagreement between the results of different groups. The earliest PNR experiment was carried out on a Nb film, 5 μm thick, deposited onto a polished silicon substrate [19]. The superconducting properties of this film were found to be satisfactory, with $H_{c1} = 1.0$ kOe at $T = 5$ K and a critical temperature $T_c = 9.2$ K. From PNR a penetration depth $\Lambda = 430 \pm 40$ Å at 4.6 K was obtained and the temperature variation of Λ was found to be consistent with a zero-temperature value $\Lambda(0) = 410 \pm 40$ Å. This value is in excellent agreement with theoretical calculations and most of other, less direct measurements. However, independent measurements from another group [20] gave different results: at $T = 4.9$ K, for a film 7000 Å thick the penetration depth was found to be $\Lambda = 900 \pm 100$ Å; for a second film, 2550 Å thick, $\Lambda = 1450 \pm 150$ Å.

Even larger discrepancies marred the determination of the penetration depth of the high-T_c superconductor $YBa_2Cu_3O_{7-x}$. The first measurement, made on a syntered pellet [21], gave a penetration depth $\Lambda = 225$ Å, a value unexpectedly low for a material with a very short coherence length and hence a large penetration depth. For two other measurements the sample was a thin film deposited epitaxially onto a substrate of $SrTiO_3$. In both cases the c-axis of the $YBa_2Cu_3O_{7-x}$ lamellar structure was perpendicular to the film and the penetration depth was measured with the magnetic field applied parallel to the surface. The two results, $\Lambda = 1400$ Å [22] and $\Lambda = 900$ $(+600, -250)$ Å [23], are in substantial agreement with each other and with the values obtained by muon resonance. All the measurements on superconductors were plagued by the presence of a sizeable surface roughness, which not only causes the 'surface' to be ill-defined but that – at least in the extreme case – may cause a shortcircuit of the magnetic flux.

What is the functional dependence of the magnetic field close to the surface of a supercon-

ductor? Provided that electronic response is entirely local, the magnetic field decays exponentially in the material [18]. Nonlocality is predicted to have visible effects only in the case of 'extreme' type I superconductors. A careful study of films of pure lead and Pb–Bi alloys was made to explore this point [24]. Pure lead is a type-I superconductor for which H_{c1} equals the thermodynamic critical field H_c. Adding an impurity level of 0.8% Bi brings the system to just below the crossover point to type-II, where H_{c1} and H_{c2} separate and the region in between is characterized by the mixed state.

The polarization of Pb(Bi) at $T = 6$ K is presented in fig. 3. The sample, in a field $H =$ 323 Oe, is in the Meissner state. The polarization appears to be entirely negative, for the following

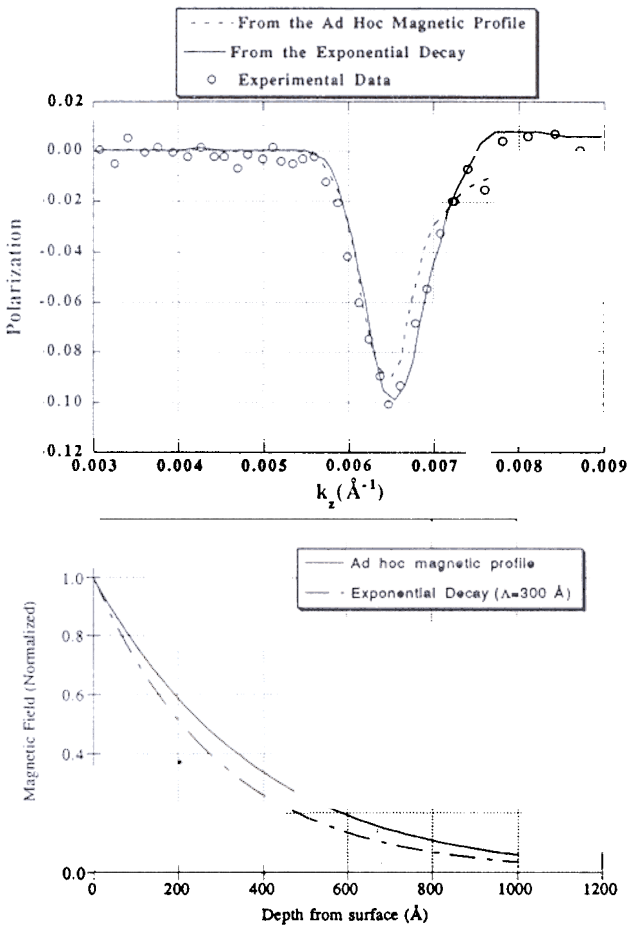

Fig. 3. Above: polarization of a film of Pb(Bi) in a field of 323 Oe and 5.5 K. The dashed line is calculated for an exponential decay of the magnetic field in the material, with a penetration depth of 300 Å. The continuous line is obtained for the parametric model profile shown below (see ref. [24]).

reason. In vacuum the magnetic induction $\boldsymbol{B}$ reduces to $\boldsymbol{H}$. Hence the discontinuity of the interaction potential at the surface is $\boldsymbol{\mu}_n \cdot (\boldsymbol{B}_{\|} - \boldsymbol{H})$: in a diamagnetic material, such as a superconductor, the neutron sees a negative magnetic field. The polarization of the Pb(Bi) film at 323 Oe is compared with the results of different calculations. If for a magnetic profile an exponential decay is adopted, certain features of the polarization are not satisfied: for instance, with an exponential decay length of 260 Å, the minimum is matched but not the values of the polarization for higher values of k_z. Much better fit is obtained with a magnetization profile that decays from the surface first less rapidly, then more rapidly an exponential function (fig. 3). Such behavior might be explained in terms of nonlocal effects; however it is hard to justify the persistance of these effects in such a 'dirty' superconductor. New independent measurements [25] are now in progress to verify these finding and also to expand earlier observations of a superconducting surface sheath predicted to occur at the superconductor/vacuum interface in these materials at higher magnetic fields.

3. Magnetic thin films

Only for film thicknesses below a few nanometers the magnetization of ferromagnetic is significantly altered from the bulk value, in size, direction of magnetization and even type of magnetic order [26]. These new properties are the result of a complex set of circumstances. Free standing films, ideally one atomic plane thick, are expected to exhibit magnetic moments larger than the bulk: since the orbital components are less quenched, the moments are expected to tend toward the free atom values. On the other hand, the lower dimensionality is expected to reduce, and even to suppress, the temperature of magnetic order. Experimental films have to be deposited on a substrate, which perturbs the magnetization of the proximate layer on two accounts. In the first place the magnetic atoms which are deposited from vapor or from a plasma arrange themselves in a structure, which tends to mimic that of the substrate.

In comparison with the bulk material, the thin film is expanded (or compressed): this may change drastically the coupling of magnetic electrons. In the second place, if both magnetic film and substrate are metallic a transfer of electrons takes place. Numerous ab initio calculations have been made for epitaxial films [27]; table 1 shows the magnetic moments predicted for one-atomic-layer-thick metals on several substrates [28].

A wealth of experimental information has been accumulated in recent years on the magnetism of thin films [29]. For instance, ultrathin films of iron have been epitaxially deposited on single crystal substrates of Cu, Ag, Au, Pd, W and MgO and studied by spin-polarized photoemission, Kerr effect, conversion electrons, Mössbauer spectroscopy and spin-polarized LEED. These studies have demonstrated the presence of ferromagnetic ordering and perpendicular surface anisotropy in monolayer thick iron films [27]. However, the determination of the absolute magnetic moment per atom of an ultra-thin film is still a tremendous challenge for experimentalists. Experiments were proposed [30] and later successfully implemented [31–35] to determine by polarized neutron reflection (PNR) the magnetic moments in Fe and Co films as thin as two monolayers. Being an optical technique, PNR goes well beyond conventional magnetometry. To start with, if the magnetic layer is covered, its depth in the sample is localized. At the same time, the optical signal assures that iron is conformed as a film, and not (for instance) in an assembly of droplets having equivalent thickness. Finally, in PNR is much easier to take into account the weak magnetic response of overlayer and substrate, even when they are much more massive than the magnetic film.

Table 1
Magnetization of thin films: theory and PNR experiments.

Monolayer	Calculated μ_B/atom	Experimental μ_B/atom	Magnetic moment in solid
Cr/Vacuum	12		:0.1
Cr/Ag		nonmagneti	:0.1
Fe/Cu		2.3	2.2
Fe/Ag	2.97		2.2
Fe/MgO	3.07	2.2	2.2
Co/Cu	1.79	1.8	1.7
Co/Ag			1.7

To perform a PNR experiment it is not necessary that the thin film is at the surface: the film may be covered with a nonmagnetic layer, which could be a few hundred Ångstroms thick. Actually such coverage *enhances* [30] the spin dependence of the reflectivity. However, the polarization is proportional to the linear magnetic flux, i.e. the product of the internal field and iron thickness ($B\,d_{Fe}$). To the extent that $k_z \cdot d_{Fe} \ll 1$, the experiment is insensitive to the variation of B within the layer, or for that matter to the thickness of the layer itself. Once known B, the mean magnetic moment per atom μ_F can be obtained with precision without detailed knowledge of the number of magnetic atoms in the layer or their density. This is because the optical potential of eq. (1) can be shown [1] to be proportional to $(b \pm c'\mu_F)N$, where c' is a constant ($c' = 0.02695 \times 10^{-12}$ cm/μ_B) and N is the atomic density per unit volume. The simultaneous fitting of $|R_+|^2$, $|R_-|^2$ strongly constrains the ratio between atomic moment of an atom and its well-known neutron scattering length.

The first magnetic thin film studied by PNR was face-centered-cubic (FCC) cobalt on Cu(0 0 1), overcoated with copper [31]. For a film 18 Å thick it was found an in-plane magnetization of $1.8\mu_B$/Co, slightly larger than the bulk value ($1.6\mu_B$). Subsequent measurements [32, 33] on even thinner films of FCC cobalt on Ag indicated a moment enhancement up to $2.15\mu_B$/Co. Although these measurements were taken at 4.2 K, the cobalt magnetization was found to be virtually unchanged up to room temperature. The behavior of thin films of body-centered iron was entirely different. A 14 Å film sandwiched in copper was fitted [31] with $2.2\mu_B$/Fe, a value virtually undistinguishable from that of the bulk. Even for a 4.3 Å film (on a rather rough surface) the ferromagnetic moment did not exceed $2.35\mu_B$/Fe at liquid helium temperature [15]. A systematic study of BCC iron films 4, 6, 8, 16 Å thick on MgO and capped with gold [35] showed a dramatic decrease of the

ordering temperature, and a concurrent change of the perpendicular anisotropy for thicknesses ≤ 6 Å; however, the ferromagnetic moment at saturation remains $(2.2 \pm 0.2)\mu_B$/Fe down to the thinnest sample (figs. 4, 5). Finally, films of Cr (down to submonolayer thickness) [33], deposited on Ag(0 0 1), did not show any measurable induced magnetization, in fields up to 0.83 kOe.

Table 1 shows a compendium of the experimental results hitherto obtained and compares them with theoretical predictions. The magnetic moments, as determined by PNR at different laboratories, are entirely consistent: however, they are very close to the bulk value and do not show the enhancement predicted for thin film materials. For Cr, the calculation is in the limit of the single atomic plane and the moments of a second plane are thought to be coupled antiferromagnetically to the first. However, the discrepancy between theory and experiment is clear and strong in the case of BCC iron, which should have enhanced magnetic moment in thin films on a number of different substrates. It is to be hoped that future experiments clarify this important point. Looking farther in the future, good ferromagnetic thin films may become useful to test in detail the properties of the phase transition in truly two-dimensional systems.

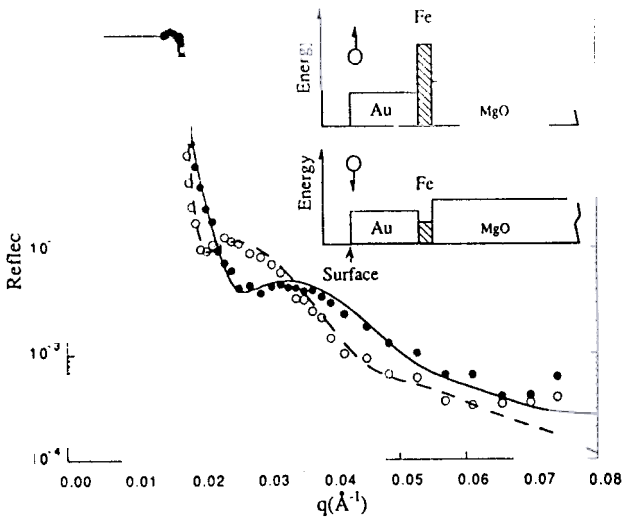

Fig. 4. Spin-dependent reflectivity of a 16 Å thick Fe film. The data were obtained at room temperature in a magnetic field of 200 Oe. Solid dots indicate data for neutron spin parallel to the applied field (+); open circles for spins antiparallel to the field (−). The insert is the schematic diagram of the neutron potential for + and − spin neutrons through the sample (see ref. [35]).

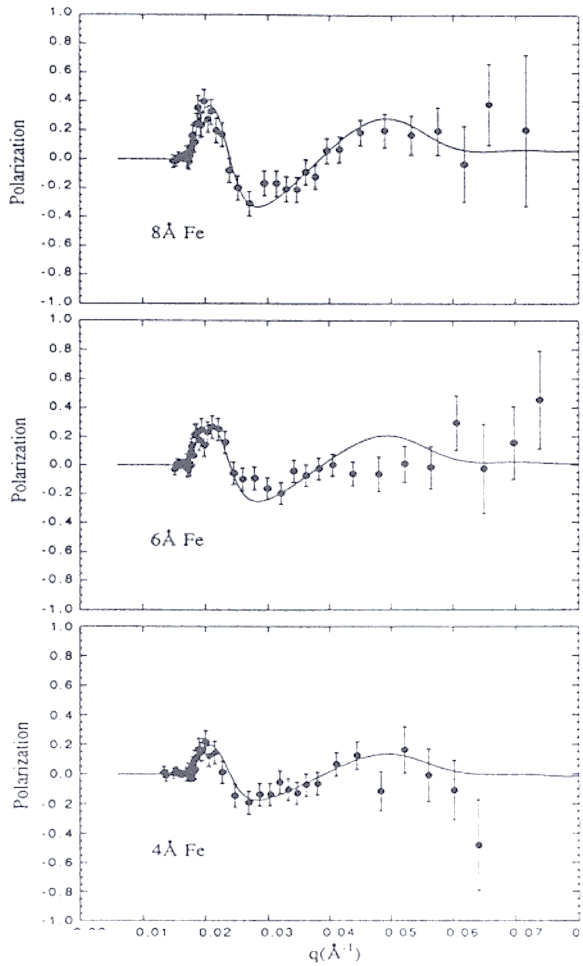

Fig. 5. Polarization functions for (bottom) 4 Å, (middle) 6 Å and (top) 8 Å Fe films at $T = 40$ K and $H = 5$ kOe. All fits used the same parameters except for the iron thickness (see ref. [35]).

4. Magnetic coupling in multilayers

The development of reliable and controlled deposition techniques has made possible the fabrication of metallic multilayers formed by interleaving ferromagnetic films with nonmagnetic spacers. The original goal of this research was to manufacture materials with novel magnetic properties just stacking conventional metals in layers of controlled thickness. First for very selected couples, then for a rapidly expanding host of combinations it was found that the

coupling between subsequent ferromagnetic layers oscillates from ferromagnetic to antiferromagnetic to ferromagnetic again as the thickness of the nonmagnetic spacers is increased. The nature of the coupling, *inferred* from the magnetization measurements, was first directly observed by neutron reflection. In all recorded cases the alignment of the magnetization of the subsequent layer was either ferromagnetic (F) or antiferromagnetic (AF) of the type + − + −, with a simple doubling of the chemical periodicity.

The first material to exhibit oscillatory magnetic interaction was a gadolinium/yttrium superlattice, epitaxialy grown on tungsten with the hexagonal *c*-axis perpendicular to the surface. When the yttrium spacer is ten atomic layers thick the superlattice is AF, as confirmed by polarized neutron diffraction [36]. A weak magnetic field in the surface plane has the effect of slightly canting the AF structure, with the main AF component perpendicular to the field. When the yttrium thickness is increased to twenty atomic planes, or decreased to six, the material becomes ferromagnetic. The oscillatory behavior has been well explained in terms of a Ruderman–Kittel–Kasuya–Yosida (RKKY) model [37]. The basic assumption is that the conduction electrons of Y provide an indirect coupling between the gadolinium layers. Since those first experiments, the studies have greatly expanded to cover other rare earths and other spacers [38].

The magnetic coupling is oscillatory also in multilayers of Fe, Co, Ni interleaved by most of the 3, 4, 5 d nonmagnetic metals. Among these, the first to be studied were multilayers of iron/chromium [39,40,41]. The magnetic fields needed to saturate the samples were found to vary periodically with the chromium thickness. The presence of an AF ground state for multilayers with high saturating fields was quickly confirmed [42,43] by PNR. The only magnetic structures found up to now in this system are of the F and the AF kind: the latter configuration is destroyed by applying a sufficiently large magnetic field (see fig. 6). Similar findings were found for other kind of multilayers, such as

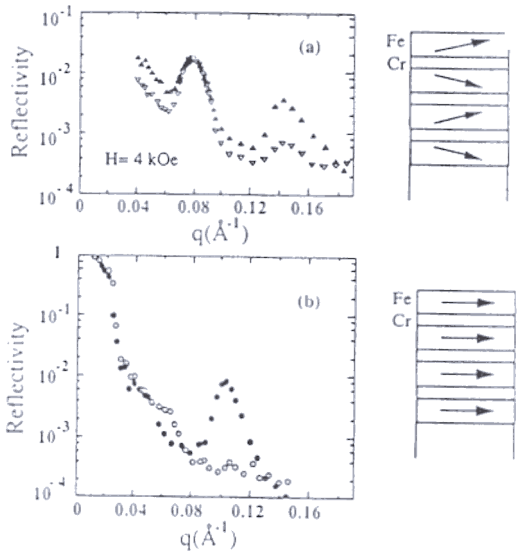

Fig. 6. (a) PNR of $\{Fe(32\,Å)/Cr(10\,Å)\}_{20}$ in a magnetic field of 4 kOe. Solid triangles: spin +. Open triangles: spin −. The magnetic moments of the Fe layers are canted, and the AF component gives rise to the spin-independent peak at $q = 0.08$ Å^{-1}, the F component to the peak at $q = 0.143$ Å^{-1}. (b) Effect of the magnetic field on the AF peak of $\{Fe(20\,Å)/Cr(10\,Å)\}_{20}$. Solid dots: spin averaged reflectivity at $H = 4$ kOe. A field of 14 kOe saturates the sample, causing the disappearance of the AF peak at $q = 0.11$ Å^{-1} (open dots) (see ref. [43]).

Co/Ru [44], Ni/Ag [45], Co/Cu [46] and Fe/Nb [47]. In the case of Fe/Si, F to AF oscillations were found to be present only for short Si thicknesses, when silicon forms a crystalline, metallic silicide. For thicknesses larger than 20 Å silicon is deposited as an amorphous semiconductor which, unless excited, does not provide magnetic coupling to the adjacent iron layers.

In retrospect, polarized neutron reflection had only a marginal role in the study of the magnetic multilayers formed by transition metals. Actually the presence of an AF or an F state is now observable in direct space by means of scanning electron microscopy with polarization analysis [49] as well as by magnetooptic Kerr effect microscopy. However, neutron measurements contain a wealth of information that reaches far beyond proving the nature of the ground state. From the intensities of the series of superlattice peaks up to large scattering angle, and of their spin dependence, one can obtain a detailed profile of the magnetization within the single

magnetic layer, with a resolution that might approach the interatomic spacing [38]. While experiments at large k_z are considered more properly in the area of conventional polarized neutron diffraction, even observations at small k_z, i.e. in the region where the mean refractive index of the material cannot be neglected, yield information that is far beyond the mere determination of the F or AF state.

As already discussed the analysis of the polarization of the reflected neutrons can be used to determine the *direction* of the magnetization at any depth in the sample. The simplest arrangement consists in analyzing the neutron spin in reference to the quantization axis of the neutrons before hitting the surface. The non-spin-flip reflectivity is due to the projection of the sample's magnetization on the quantization axis, while the spin-flip reflectivity is due to the perpendicular component of the magnetization. In this way the presence of a canted arrangement of spins has been observed first in Gd/Y [36] and later in Fe/Cr [42]. A more quantitative comparison of $|R_{++}|^2$, $|R_{+-}|^2$, $|R_{-+}|^2$ and $|R_{--}|^2$ has been done for Co/Cu [46]. Polarization analysis is also been used [50] to search for direct evidence of a magnetic state where two magnetic layers of a sandwich are magnetized at a 90° angle, rather than at 0° or 180°. The presence of such a state has been inferred from magnetic measurements, and it is justified if biquadratic terms in the magnetic exchange become important [51].

Polarization analysis becomes important to sort out the structures of more complex artificial superlattices, as those made by the alternation of two magnetic metals. Prototype of this class is a Gd/Fe multilayer, a material for which model properties have been proposed [52] and presently tested. This material is made of two magnetic components, Gd and Fe, which are antiparallel to each other but have in general different sizes. In an applied magnetic field the magnetic structure is predicted to transform from a ferrimagnetic to a 'twisted' configuration. This is composed of an antiferromagnetic component perpendicular to the field and a ferromagnetic component, unequal for the two components, parallel to the field. Since the magnetic coupling is weaker for the surface layer, it has been suggested that the phase transformation in a magnetic field should initiate at the surface, and its character should depend on the nature of the surface layer [52]. Experiments now in progress [53,54] tend to confirm in real samples the main features of the mean field model.

Up to now it was implicitly assumed that the sample is composed of a single domain. In this case the reflected neutrons are not depolarized (even from nonuniaxial samples) but at most the direction of their spins change from the initial polarization axis. In principle the reference field for polarization analysis can be rotated until parallel to the quantization axis of the exiting neutrons: the spin-flip components of the reflectivity become identically zero. If a device capable of providing 'flexible' polarization analysis were constructed [55], it would also discriminate the case discussed above from that, in which more than one magnetic domain is present in the sample. Here, since different neutrons experience different magnetic pathways, the reflected beam is truly depolarized. Magnetic domains have an additional effect: the magnetism is no longer uniform in the plane of the film, and the finite size of the domains gives rise to scattering around the direction of the reflected beam.

5. Forward magnetic scattering

In order to measure the reflected beam suffices a single counter, poised at an angle θ with the reflecting surface, and 2θ with the primary beam. However, in several instruments a one-dimensional, position sensitive detector is used, with the geometry sketched in fig. 7. Such detectors offer several practical advantages: the reflected beam is easily localized and both signal and background are measured at the same time. More important, these detectors measure not only reflected neutrons, but also those scattered at grazing incidence. Notice that in the geometry shown in fig. 7 a one-dimensional detector discriminates only neutrons leaving the surface at

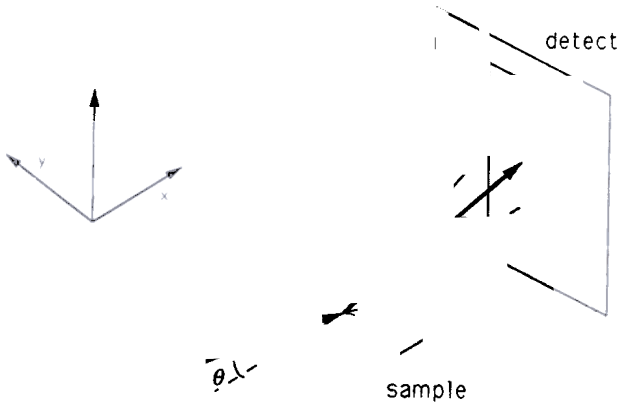

Fig. 7. Geometry of forward and lateral scattering of neutrons at grazing incidence.

an angle θ_f different from θ_i; however, the scattering always takes place in the plane of reflection. In contrast, in the most common geometry of scattering at grazing incidence [56], the observations are focussed on the neutrons scattered *out* of the reflection plane. There is an important difference between the two cases, and thus to avoid confusion I will name the scattering in the plane of reflection as '*forward* scattering' to distinguish it from the lateral scattering at grazing incidence.

In both cases the scattering is due to dishomogeneities in the plane of the film, which might be represented by a vector τ with planar projections τ_x and τ_y (fig. 8). In the forward scattering τ_x is obtained from the separation $\Delta\theta$ between the scattered and the reflected beam. In the lateral scattering τ_y is obtained from the angle $\Delta\phi$ between the scattered beam and the reflection plane. When τ is small in comparison with the incoming wavevector, the laws of conservation of energy and momentum in plane reduce to:

$$\tau_x = |k| \sin\theta \, \Delta\theta$$
$$\tau_y = |k| \, \Delta\phi \qquad (|k| = 2\pi/\lambda) \tag{6}$$

For comparable elements $\Delta\theta, \Delta\phi$ the regions of τ_x, τ_y are entirely different. For instance, if $\Delta\theta =$

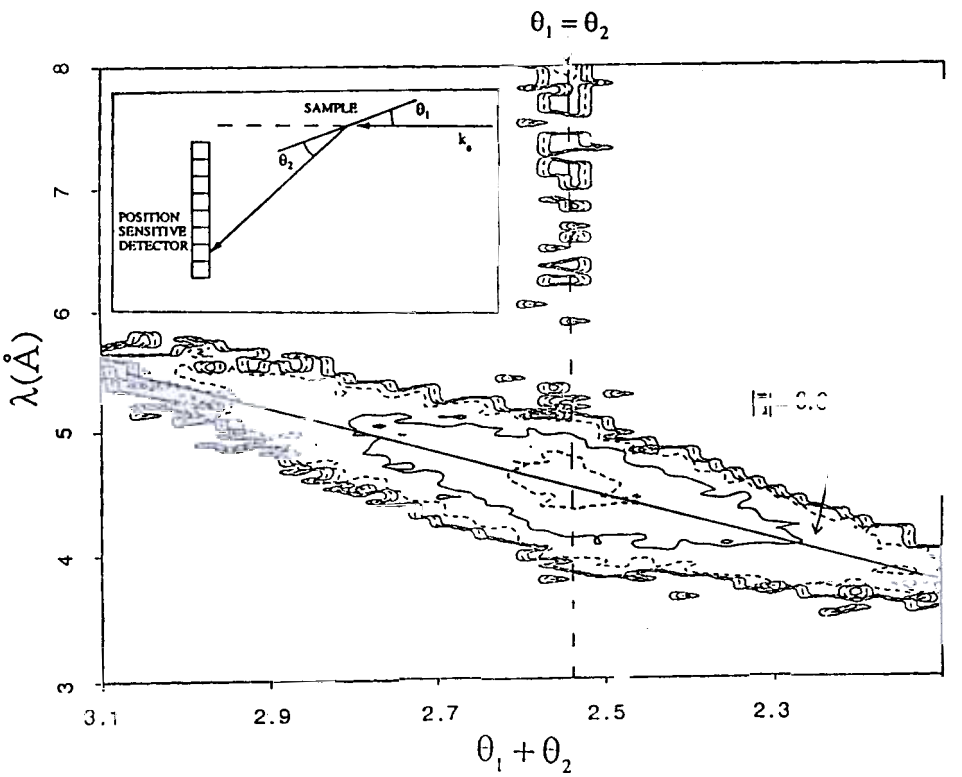

Fig. 8. Intensity contour of a Co/Ru multilayer (from ref. [44]). The locus of the reflected beam is a vertical line at $\theta_1 = \theta_2$. The forward scattering ridge is at $|q| = \tau_x$, centered around the AF peak.

$\theta = \Delta\phi = 1°$, and a neutron wavelength $\lambda = 10$ Å, $\tau_x = 1.9 \times 10^{-4}$ Å^{-1}, while $\tau_y = 1.1 \times 10^{-2}$ Å^{-1}. The difference is about of two orders of magnitude. This means that, if the lateral fluctuations τ are isotropic in the plane of the film ($\tau_x = \tau_y$) scattering might be present at a detectable $\Delta\theta$ even when $\Delta\phi$ is negligibly small. The size of the objects that give rise to lateral scattering is the same as that giving rise to small angle scattering in transmission geometry: it is of order of 100 Å. The fluctuations that give rise to observable forward scattering are instead of the order of one micron.

Sizeable forward scattering has been observed in several instances, when reflectivity measurements were taken on magnetic multilayers. In fig. 8 is shown an intensity contour pattern obtained for a Co/Ru multilayer [44], and in fig. 9 that for a Fe/Nb multilayer [47]. The measurements were done at a pulsed neutron source, where the intensity reflected at a given angle with respect to the primary beam, $\theta_i + \theta_f$, are measured for all neutron wavelengths. In this pattern, the reflected beam appears as a vertical line of intensity at $\theta_i = \theta_f$. The visible scattering

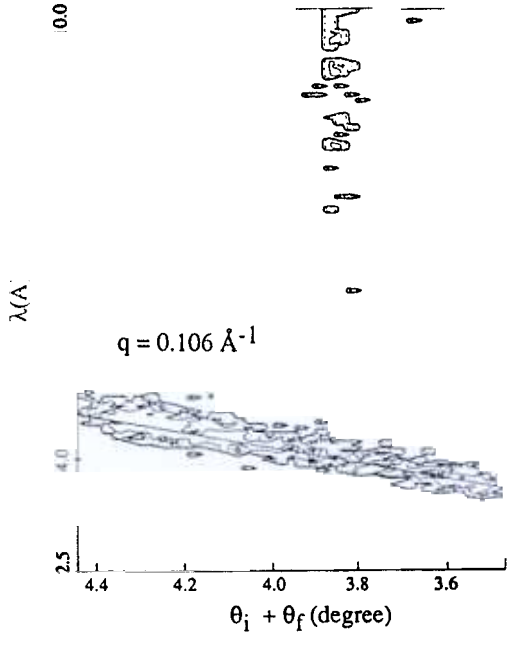

Fig. 9. Forward scattering of a Fe/Nb multilayer (from ref. [47]). The forward scattering is much broader than the dimension of the counter (2.5 cm, at 90 cm from the sample).

has the form of a ridge centered around a value of $|q|$ equal to the value of the maximum of the AF peak, i.e. where $q_z = \tau_z$, τ_z being the propagation vector of the antiferromagnetic structure. In contrast, at the first Bragg reflection due to chemical modulation of the multilayer no corresponding broadening is present. The forward scattering is of magnetic origin: it is as if the antiferromagnetic domains had finite size. It is easy to form a picture of the configuration, by assigning to each domain a magnetization axis, which may point along a local crystallographic axis.

It is easy to calculate the lateral dimensions of the domains observed for Co/Ru with the help of a simple formula. In the kinematic approximation the intensity of the antiferromagnetic peak [57] may be written as

$$= J_z J_x = \frac{\sin^2(N_z ak \sin\theta \cos\alpha)}{\sin^2(ak \sin\theta \cos\alpha)} \frac{\sin^2(N_x ak \sin\theta \sin\alpha)}{\sin^2(ak \sin\theta \sin\alpha)} \qquad 7$$

where we have neglected fluctuations along y. In eq. (7), a is the antiferromagnetic spacing and N_z is the number of layers composing the film. In J_x, a is in reality a dummy parameter; what is of interest is the total length $L_x = N_x a$ in the x direction. α is the angle between the scattering vector and the z-direction: at the Bragg reflection $\alpha = 0$ and the arguments in J_z are multiples of 2π. When the incident wavevector $k = 2\pi/\lambda$ is changed (but the angle of incidence θ remains constant) the maximum of J_z occurs for finite α: it is easy to see that under this condition q_z remains constant. At finite α, J_x rapidly decreases; L_x may be chosen by finding the value of α at which $J_x = 0$. From fig. 8 it may be deduced that, for Co/Ru, $L_x \simeq 4$ μm. In the case of Fe/Nb (fig. 9) the counter used is too limited to give an estimate of the size of L_x and only an upper limit can be given: $L_x < 0.6$ μm.

In conclusion, in the past ten years PNR has been developed into a mature technique which is being employed to study a variety of magnetic phenomena in samples having lamellar geome-

try. At the same time, the development of (lateral) scattering at grazing incidence, as well as that of forward scattering, may open new and exciting areas of research.

Acknowledgements

The present work was supported by the US Department of Energy, BES-Material Sciences, under contract W-31-109-ENG-38. The author would like to thank Prof. W.G. Stirling for giving him the opportunity to present this work at the ILL-ESRF Workshop on Neutrons and X-rays in Magnetism. The author is also grateful to R. Goyette and Y.Y. Huang for their help in preparing the figures, and to Hong Lin for a critical reading of the manuscript.

References

[1] D.J. Hughes, Pile Neutron Research (Addison-Wesley, Cambridge, 1953).
[2] G.P. Felcher, R.O. Hilleke, R.K. Crawford, J. Haumann, R. Kleb and G. Ostrowski, Rev. Sci. Instrum. 58 (1987) 609.
[3] S.J. Blundell and J.A.C. Bland, Phys. Rev. B 46 (1992) 3391.
[4] G.P. Felcher, Proc. S.P.I.E. 983 (1989) 2.
[5] G.P. Felcher, Y.Y. Huang, M. Carey and A. Berkowitz, in: Proceedings of the Symposium on Ultrathin Films Multilayers and Surfaces, Lyon, September 1992, J. Magn. Magn. Mater. 121 (1993) 105.
[6] J. Lekner, Theory of Reflection (Martinus Nijhoff, Dordrecht, 1987).
[7] M. Klibanov and P.E. Sacks, J. Math. Phys. 33 (1992) 3813.
[8] J.S. Pedersen, J. Appl. Cryst. 25 (1992) 129.
[9] S.S.P. Parkin, V.R. Deline, R.O. Hilleke and G.P. Felcher, Phys. Rev. B 42 (1990) 10583.
[10] C.F. Majkrzak, Physica B 173 (1991) 75.
[11] R. Felici, J. Penfold, R.C. Ward and W.G. Williams, Appl. Phys. A 45 (1988) 169.
[12] M. Maaza, in: Proceedings of the International School of Physics Enrico Fermi, Course CXIV, eds. M. Fontana and F. Rustichelli (North-Holland, Amsterdam, 1992) p. 341.
[13] D.A. Korneev, V.V. Pasyuk, A.V. Petrenko and E.B. Dokukin, Springer Proc. Phys. 61 (1992) 213.
[14] S.S.P. Parkin, R. Sigsbee, R. Felici and G.P. Felcher, Appl. Phys. Lett. 48 (1986) 604.
[15] J.A.C. Bland, A.D. Johnson, H.J. Lauter, R.D. Bateson, S.J. Blundell, C. Shakleton and J. Penfold, J. Magn. Magn. Mater. 93 (1991) 513.
[16] G.P. Felcher, Phys. Rev. B 24 (1981) 1595.
[17] K. Tulipan, Diplomarbeit, Ludwigs-Maximilians-Universität München, September 1991.
[18] M. Tinkham, Introduction to Superconductivity (McGraw-Hill, New York, 1975).
[19] G.P. Felcher, R.T. Kampwirth, K.E. Gray and Roberto Felici, Phys. Rev. Lett. 52 (1984) 1539.
[20] L.P. Chernenko, D.A. Korneev, A.V. Petrenko, N.I. Balalykin and A.S.V. Skripnik, Springer Proc. Phys. 61 (1992) 209.
[21] R. Felici, J. Penfold, R.C. Ward, E. Olsi and C. Matacotta, Nature 329 (1987) 523.
[22] A. Mansour, R.O. Hilleke, G.P. Felcher, R.B. Laibowitz, P. Chaudhari and S.S.P. Parkin, Physica B 156 (1989) 867.
[23] S.V. Gaponov, E.B. Dokukin, D.A. Korneev, E.B. Kluenkov, W. Loebner, V.V. Pasyuk, A.V. Petrenko, H. Rzany and L.P. Chernenko, Pis'ma Zh. Eksp. Teor. Fiz. 49 (1989) 277.
[24] K.E. Gray, G.P. Felcher, R.T. Kampwirth and R. Hilleke, Phys. Rev. 42 (1990) 3971M.
[25] A.T. Boothroyd, D.McK. Paul, M.P. Nutley and J. Penfold, ISIS Experimental Report 1992, A 164.
[26] R.E. Watson, P. Fulde and A. Luther, AIP Conf. Proc. 10 (1972) 32 and references therein.
[27] L.M. Falicov, D.T. Pierce, S.D. Bader, R. Gronsky, K.L. Hathaway, H.J. Hopster, D.N. Lambeth, S.S.P. Parkin, G. Prinz, M. Salamon, I.K. Schuller and R.H. Victora, J. Mater. Res. 5 (1990) 1299.
[28] A.J. Freeman, A. Continenza and Chun Li, Mater. Res. Sci. Bull. XV(9) (1990) 27.
[29] Landoldt-Bornstein, Magnetic Properties of Metals: Thin Films, Vol. 19, ed. H.P.J. Vijn (Springer-Verlag, Berlin, 1988).
[30] G.P. Felcher, K.E. Gray, R.T. Kampwirth and M.B. Brodsky, Physica B 136 (1986) 59.
[31] J.A.C. Bland, D. Pescia and R.F. Willis, Phys. Rev. Lett. 58 (1987) 1244.
[32] H.J. Lauter, J.A.C. Bland, R.D. Bateson and A.D. Johnson, Springer Proc. Phys. 61 (1992) 219.
[33] J.A.C. Bland, R.D. Bateson, A.D. Johnson, B. Heinrich, Z. Celinski and H.J. Lauter, J. Magn. Magn. Mater. 93 (1991) 331.
[34] J.A.C. Bland, R.D. Bateson, P.C. Ried, R.G. Graham, H.J. Lauter, J. Penfold and C. Shackleton, J. Appl. Phys. 69 (1991) 4989.
[35] Y.Y. Huang, C. Liu and G.P. Felcher, Phys. Rev. B 47 (1993) 183.
[36] C.F. Majkrzak, J.W. Cable, J. Kwo, M. Hong, D.B. McWhan, Y. Yafet, J.V. Waszczak and C. Vettier, Phys. Rev. Lett. 56 (1986) 2700.
[37] Y. Yafet, J. Appl. Phys. 61 (1987) 4058.
[38] C.F. Majkrzak, J. Kwo, M. Hong, Y. Yafet, D. Gibbs, C.L. Chien and J. Bohr, Adv. Phys. 40 (1991) 99.
[39] P. Gruenberg, R. Schreiner, Y. Pang, M.B. Brodsky and H. Sowers, Phys. Rev. Lett. 57 (1986) 2442.

[40] M.N. Baibich, J.M. Broto, A. Fert, F. Nguyen van Dau, F. Petroff, P. Etienne, G. Creuzet and A. Friederich, Phys. Rev. Lett. 61 (1988) 2472.
[41] S.S.P. Parkin, N. More and K.P. Roche, Phys. Rev. Lett. 64 (1990) 2304.
[42] A. Barthelemy, A. Fert, M.N. Baibich, S. Hadjoudj, F. Petroff, P. Etienne, R. Cabanel, S. Lequien, F. Nguyen van Dau and G. Creuzet, J. Appl. Phys. 67 (1990) 5908.
[43] S.S.P. Parkin, A. Mansour and G.P. Felcher, Appl. Phys. Lett. 58 (1991) 1473.
[44] Y.Y. Huang, G.P. Felcher and S.S.P. Parkin, J. Magn. Magn. Mater. 99 (1991) L31.
[45] B. Rodmacq, P. Mangin and C. Vettier, Europhys. Lett. 15 (1991) 503.
[46] A. Screyer, T. Zeidler, Ch. Morawe, N. Metoki, H. Zabel, J.F. Ankner and C.F. Majkrzak, J. Appl. Phys., to be published.
[47] J.E. Mattson, E.E. Fullerton, C.H. Sowers, Y.Y. Huang, G.P. Felcher and S.D. Bader, in: 37th Conf. on Magn. and Magn. Mat., J. Appl. Phys. 73 (1993) 5969.
[48] E.E. Fullerton, J.E. Mattson, S.R. Lee, C.H. Sowers, Y.Y. Huang, G.P. Felcher, S.D. Bader and F.T. Parker, J. Magn. Magn. Mater. 117 (1992) L301.
[49] J. Unguris, R.J. Celotta and D.T. Pierce, Phys. Rev. Lett. 67 (1991) 140.
[50] A. Schreyer, K. Bröhl, Th. Zeidler, Ch. Morawe, N. Metoki, H. Zabel, J.A. Wolf, P. Grünberg, J.F. Ankner and C.F. Majkrzak, presented at Intern. Workshop on the Use of Neutrons and X-Rays in the Study of Magnetism, Grenoble, January 1993.
[51] J.C. Slonczewski, Phys. Rev. Lett. 67 (1991) 3172.
[52] J.G. LePage and R.E. Camley, Phys. Rev. Lett. 65 (1990) 1152.
[53] C. Dufour, Ph. Bauer, M. Sajieddine, K. Cherifi, G. Marchal and Ph. Mangin, J. Magn. Magn. Mater. 121 (1993) 300.
[54] M. Löwenhaupt, W. Hahn, Y.Y. Huang, G.P. Felcher and S.S.P. Parkin, J. Magn. Magn. Mater. 121 (1993) 173.
[55] P.J. Brown, Physica B 192 (1993) 14.
[56] H. Dosch, Physica B 192 (1993) 163.
[57] R.W. James, The Optical Principles of Diffraction of X-Rays (Cornell University Press, Ithaca, 1962).